Visual Functional and Histopathological Correlation in Experimental Autoimmune Optic Neuritis

Yoshimichi Matsunaga,[1] *Takeshi Kezuka,*[1] *Xiaoming An,*[1] *Kouji Fujita,*[2] *Nagahisa Matsuyama,*[2] *Ryusaku Matsuda,*[1] *Yoshihiko Usui,*[1] *Naoyuki Yamakawa,*[1] *Masahiko Kuroda,*[2] *and Hiroshi Goto*[1]

Purpose. To elucidate the correlation between visual threshold of optokinetic tracking (OKT), visual evoked potential (VEP), and histopathology at different time points after induction of experimental autoimmune optic neuritis (EAON).

Methods. EAON was induced in C57BL/6 mice by subcutaneous immunization with an emulsified mixture of myelin oligodendrocyte glycoprotein $(MOG)_{35-55}$ peptide. OKT and VEP were measured on days 7, 14, 21, 28, and 42 postimmunization. After VEP measurements, the mice were killed and their eyes were enucleated for histopathological studies. Immunohistochemical staining was performed using cell-specific markers for characterization of cells in the optic nerve: CD3 (T cells), Iba-1 (microglia), MBP (myelin basic protein), and neurofilament (axons).

Results. Functionally, OKT threshold decreased as early as day 7, and VEP latency was significantly prolonged on day 21. Axon degeneration was observed as early as day 14. Activated microglia infiltration was also observed on day 14, before T cell infiltration, which peaked on day 21. Demyelination, confirmed by MBP staining, was observed on day 21.

Conclusions. Microglial infiltration in the optic nerve coincided with decline in OKT threshold and preceded VEP latency prolongation, while VEP latency prolongation coincided with T cell infiltration and demyelination of the optic nerve. These findings may contribute to understanding of the pathophysiology of optic neuritis and future development of more effective therapeutic strategy for refractory optic neuritis. (*Invest Ophthalmol Vis Sci.* 2012;53:6964–6971) DOI: 10.1167/iovs.12-10559

Among patients with multiple sclerosis (MS), 38% present with optic neuritis as the initial symptom before development of subsequent neurological symptoms.[1] The pathogenesis of optic neuritis has been considered to be chronic inflammation and demyelination of the optic nerve axons with a relapsing–remitting course, eventually causing neurodegeneration as in MS.[2,3]

As a functional aspect of the optic nerve, conductivity is evaluated by visual evoked potential (VEP). Prolongation of VEP latency is presumed to represent demyelination of the axons in the optic nerve, which is followed by shortening of latency (in other words, normalization) as a result of subsiding inflammation and/or remyelination, although latency does not fully recover to normal level.[4–6] On the other hand, visual acuity of patients with optic neuritis recovers to normal level (20/20 or better) in 71% of the patients in 1 year[7] and is maintained in 72% of the patients in 15 years,[7] while VEP latency stays prolonged. This discrepancy between optic nerve conductivity and visual acuity has been reported in previous clinical studies and suggests that conductivity is not responsible for decline in visual acuity.[4,5]

Studies so far have defined the development of experimental autoimmune optic neuritis (EAON) based on histopathological findings, so-called "pathological EAON,"[8–10] and have not been able to grade visual loss or define the onset of EAON based on visual symptoms. On the other hand, in the mouse experimental autoimmune encephalomyelitis (EAE) model for MS, onset of inflammation in the spinal cord is well defined by clinical symptoms and is graded as EAE score (such as decrease in tail tone and partial paralysis of hindlimb). In addition, it is known that clinical symptoms precede histopathologically confirmed T cell infiltration into the spinal cord, causing demyelination.[11,12]

Optokinetic head tracking (OKT) threshold is an objective assessment of visual acuity similar to optokinetic nystagmus in humans. Instead of by nystagmus, as in humans, OKT is evaluated by head movement in mice.[13–15] In humans, researchers have used optokinetic nystagmus to assess objective visual acuity under different conditions[16] and in different ocular diseases,[17] and the clinical significance is well established.

In the present study, we used OKT threshold and VEP to evaluate visual function in the mouse EAON model and correlated the findings with optic nerve pathology at different time points.

Materials and Methods

Mice

C57BL/6 mice were purchased from the Central Institute for Experimental Animals (Tokyo, Japan) and were maintained in specific pathogen-free conditions at Tokyo Medical University, Japan. All experiments were approved by the Institutional Animal Research

From the Departments of [1]Ophthalmology and [2]Molecular Pathology, Tokyo Medical University, Shinjuku-ku, Tokyo, Japan.

Supported by Grant-in-Aid (C) for Scientific Research from the Japan Society for the Promotion of Science and a follow-up grant for Tokyo Medical University research project.

Submitted for publication July 10, 2012; revised August 30, 2012; accepted September 6, 2012.

Disclosure: **Y. Matsunaga**, None; **T. Kezuka**, None; **X. An**, None; **K. Fujita**, None; **N. Matsuyama**, None; **R. Matsuda**, None; **Y. Usui**, None; **N. Yamakawa**, None; **M. Kuroda**, None; **H. Goto**, None

Corresponding author: Takeshi Kezuka, Department of Ophthalmology, Tokyo Medical University, 6-7-1 Nishi-shinjuku, Shinjuku-ku, Tokyo 160-0023, Japan; tkezuka@tokyo-med.ac.jp.

Investigative Ophthalmology & Visual Science, October 2012, Vol. 53, No. 11

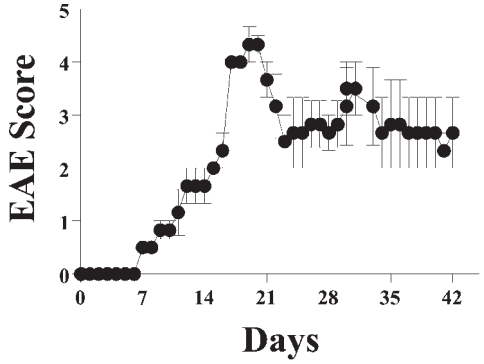

Figure 1. EAE scores during the course of disease. Mice were immunized with 300 μg of MOG_{35-55} emulsified in complete Freund's adjuvant and DMSO. EAE was scored every day ($n = 6$). Data are expressed as mean ± SEM. Similar results were obtained in two independent experiments.

Committee of Tokyo Medical University and conformed to the ARVO Statement for the Use of Animals in Ophthalmic and Vision Research.

Reagents

Myelin oligodendrocyte glycoprotein $(MOG)_{35-55}$ peptide (MEVGWYRSPFSRVVHLYRNGK) was synthesized by conventional solid-phase techniques, as described elsewhere.[8] Purified *Bordetella pertussis* toxin and dimethyl sulfoxide (DMSO) were from Sigma Chemical (St. Louis, MO). Complete Freund's adjuvant (CFA) and *Mycobacterium tuberculosis* strain H37Ra were from Difco (Detroit, MI).

EAON Induction and EAE Score

The method of EAON induction has been discussed in detail previously.[18] Briefly, mice were immunized with 300 μg of MOG_{35-55} emulsified in CFA and DMSO into the nape of the neck. *Bordetella pertussis* toxin (1 μg/mouse) was also injected intraperitoneally on the day of immunization. EAE was scored every day ($n = 36$). Clinical EAE scores are as follows: 0, no deficit; 0.5, partial decrease in tail tone; 1, decreased tail tone; 2, hindlimb weakness or partial paralysis; 3, complete hindlimb paralysis; 4, forelimb weakness and hindlimb paralysis; 4.5, complete forelimb paralysis in either arm and hindlimb paralysis; 5, quadriplegia.

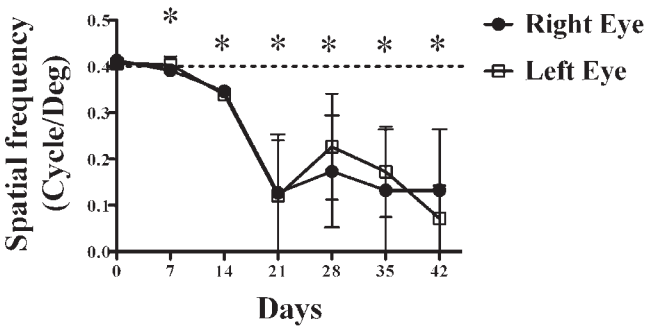

Figure 2. Changes in OKT threshold during the course of EAON. OKT threshold decreased statistically significantly from day 7 in either eye (day 0: 0.413 ± 0.005 cyc/deg versus day 7 right eye: 0.392 ± 0.005 cyc/deg), and bilaterally on day 14 (right eye: 0.347 ± 0.008 cyc/deg, left eye: 0.339 ± 0.009 cyc/deg) reaching to a peak at day 21 (right eye: 0.127 ± 0.103 cyc/deg, left eye: 0.120 ± 0.098 cyc/deg). *Dotted line* represents the level of spatial frequency in normal control mice (approximately 0.4 cyc/deg). Data are expressed as mean ± SEM (SEM too small to show on days 0, 7, 14) of three mice from each group. Statistical analysis was performed using Mann-Whitney *U* test. $^*P < 0.05$ compared to control. Similar results were obtained in two independent experiments.

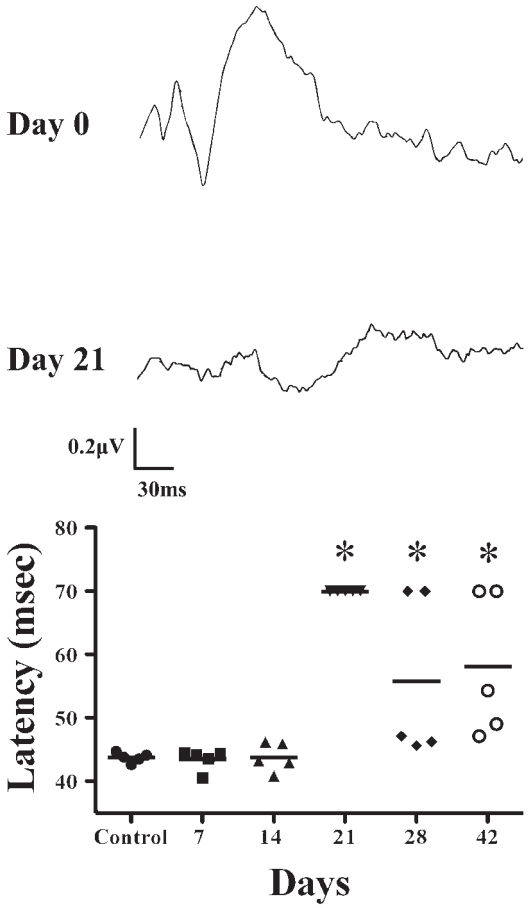

Figure 3. (*Top*) Representative VEP wave pattern of EAON. At day 21, VEP was not recordable, indicating that conductivity was severely impaired. (*Bottom*) Changes in VEP latency during the course of EAON. Latency prolongation peaked on day 21, at which point the negative wave could not be recorded in most of the mice and latency was arbitrarily assigned a value of 70 ms. After day 21, latency did recover, but not to normal levels. Values represent mean (±SD) results from five mice in each group. *Box-and-whisker plots* indicate median, range, upper quartile, and lower quartile obtained from five mice in each group. Statistical analysis was performed using Mann-Whitney *U* test. $^*P < 0.05$ compared to control. Similar results were obtained in two independent experiments.

Optokinetic Head Tracking Threshold Measurement

Optokinetic head tracking threshold is a measurement of spatial frequency threshold by observing the head movement of a mouse when tracking rotating sinusoidal gratings. This was done using a commercial apparatus, OptoMotry (Cerebral Mechanics Inc., Lethbridge, AB, Canada). The method is well established, and the methodology and theory have been discussed previously.[15] Two researchers (Y.M. and G.A.) measured the OKT threshold for each eye ($n = 6$) in a blinded fashion at different time points (before immunization; day 0; and days 7, 14, 28, and 42). Mice with an EAE score of 4.5 or above were excluded from measurement because these mice could not maintain an upright position; this would influence OKT threshold measurement since head tracking movement is disturbed by muscle weakness.

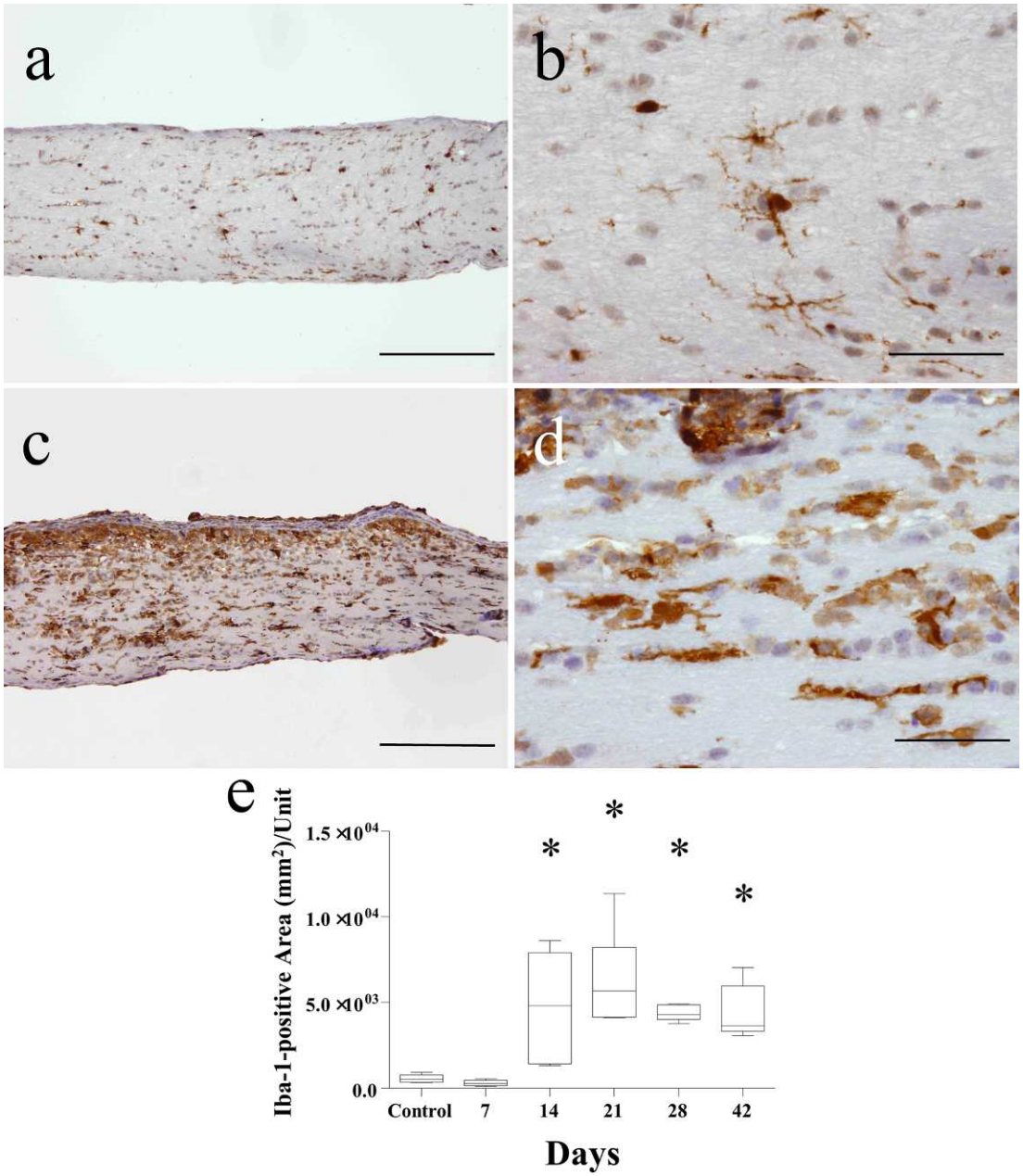

Figure 4. Immunohistochemical study of microglia (Iba-1-positive cells) in the optic nerve. (**a**) Microglia in normal optic nerve (*bar* = 100 μm). (**b**) Higher magnification of **a** showing ramified microglia (quiescent state) (*bar* = 50 μm). (**c**) Increased microglia in the optic nerve of an EAON model mouse on day 14 after immunization (*bar* = 100 μm). (**d**) Higher magnification of **c** showing amoeboid microglia (active state) (*bar* = 50 μm). (**e**) Chronological changes of Iba-1-positive area in the optic nerve. Microglial activation in optic nerve occurred as early as day 14. *Box-and-whisker plots* indicate median, range, upper quartile, and lower quartile obtained from five mice in each group. Statistical analysis was performed using Mann-Whitney *U* test. $^*P < 0.05$ compared to control.

Photopic Flash VEP Recording

One day before VEP measurement, a stainless steel screw was inserted into the right half of the skull of a mouse corresponding to the visual cortex (1.5 mm laterally to the midline, 1.5 mm anterior to the lambda) as a measuring electrode.[19] On the day of recording, the mouse was anesthetized with an intraperitoneal injection of a mixture of ketamine (80 mg/kg) and xylazine (8 mg/kg). The right eyelid was closed using black vinyl tape, and the left eye was stimulated by a commercial Gantzfeld stimulator (Kowa, Tokyo, Japan) and bandpass filtered and amplified (Neuropack μ, MEB9104; Nihon Kohden, Tokyo, Japan). Stimulation conditions are as follows: stimulation intensity, 0.03 cd/m^2; stimulation frequency, 0.1 Hz; band-pass filter, 1 to 200 Hz. In each mouse, 32 responses were averaged. Latency was evaluated as the major negative wave after flash stimulation. For mice in which VEP could not be recorded, latency was arbitrarily assigned as 70 ms.

Immunohistochemistry

After OKT threshold measurement, mice were anesthetized with an overdose of pentobarbiturate, and cardiac perfusion was performed with 10% neutral buffered formaldehyde. Both eyes were enucleated and immersed in the same fixative overnight. The optic nerve was

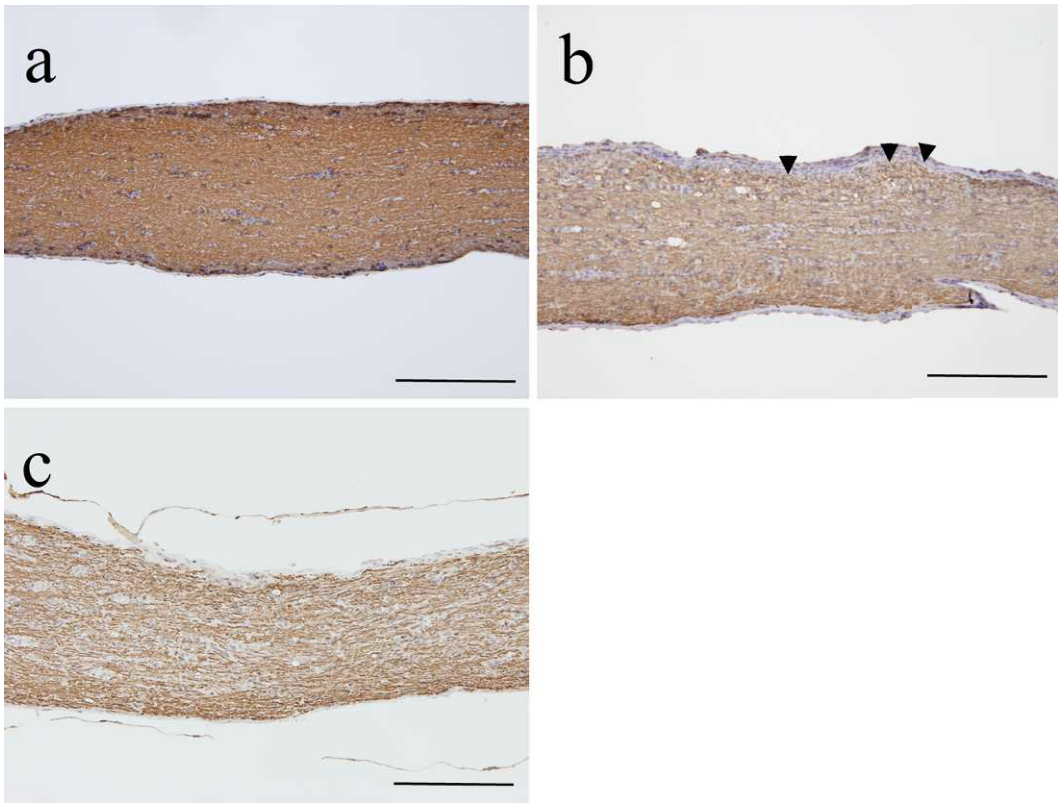

FIGURE 5. Immunohistochemical study of neurofilament in the optic nerve. (**a**) Normal optic nerve shows densely stained neurofilaments as linear structure. (**b**) Optic nerve of an EAON model mouse on day 14 after immunization. Partial irregularity of the linear structure (*arrowheads*) can be seen where cellularity (nuclei stained by hematoxylin) is high. (**c**) Irregularity of linear structure expands throughout the optic nerve. Cellularity is much higher on day 14. *Bar* = 100 μm.

resected just at the back of the globe (not including the optic chiasm). Tissues were embedded in paraffin, and 4-μm-thick sections were mounted onto New Silane III glass slides (Muto Pure Chemicals Co., Ltd., Tokyo, Japan) and dried at 60°C. Hematoxylin and eosin staining was performed to evaluate laterality and induction of EAON pathologically.

Immunohistochemical studies were performed using cell-specific markers to characterize the cells in the optic nerve: CD3 (T cells), Iba-1 (microglia), myelin basic protein (MBP; myelin), and neurofilament (axons), after immunization on day 0 and on days 7, 14, 21, 28, and 42 after immunization ($n = 5$; five nonimmunized mice were also measured as normal controls). At each time point, after VEP measurements were performed, mice were killed and the eyes were enucleated and fixed, as discussed above, for immunohistochemical studies (n = five mice at each time point). After deparaffinization in xylene and washing in graded ethanol, endogenous peroxidases were quenched with 0.3% H_2O_2 methanol for 15 minutes. Antigen retrieval was performed using a 10 M sodium citrate solution (pH 6.0) at 100°C (microwave) for 20 minutes. The following primary antibodies were used: rabbit anti-CD3 antibody (1:400; Dako Japan, Tokyo, Japan), rabbit anti-Iba-1 antibody (1:1000; Wako Chemical, Tokyo, Japan), rabbit anti-MBP antibody (1:5, Histofine kit; Nichirei, Tokyo, Japan), and antineurofilament antibody (1:400; Dako Japan). Primary antibodies were applied for 3 hours at room temperature. For secondary antibody, swine polyclonal anti-rabbit IgG (Dako Japan) was used. Horseradish peroxide (HRP)–streptavidin conjugate (Dako Japan) and 3-3′-diaminobenzidine tetrahydrochloride and HRP reaction were used for visualization. Cell nuclei were stained by hematoxylin. After immunostaining, images were acquired by a light microscope (BX50; Olympus, Tokyo, Japan) equipped with a digital camera (DP70; Olympus). The density of stained cells and the stained cell surface area per unit area (photographed at 10×, 20× objective lens magnification) were analyzed using ImageJ software (U.S. National Institutes of Health, Bethesda, MD; http://imagejnihgov/ij/).

Statistical Analysis

GraphPad Prism (GraphPad Software, San Diego, CA) was used for statistical analysis and graph generation. Mann-Whitney U test was used to compare OKT threshold, stained cell density, and stained cell surface area between EAON model mice and normal controls. Statistical significance was defined as $P < 0.05$ in all data analysis and is denoted by an asterisk in the graphs.

RESULTS

OKT Threshold Declines before VEP Latency Prolongation

For the course of EAE development, disease onset was observed after day 7 (Fig. 1). We attempted to define the development of EAON functionally by OKT threshold. There was a statistically significant decrease starting as early as day 7 in the right eye (day 0: 0.413 ± 0.005 cyc/deg versus day 7 right eye: 0.392 ± 0.005 cyc/deg) and then in both eyes on day 14 (right eye: 0.347 ± 0.008 cyc/deg, left eye: 0.339 ± 0.009 cyc/deg) (Fig. 2). On the other hand, VEP latency increased significantly from day 21 (day 0: 43.74 ± 0.69 ms, day 7: 43.40 ± 1.49 ms versus day 21: 70.00 ± 0.00 ms) (Fig. 3). Therefore, OKT threshold decrease occurred much earlier than VEP latency prolongation. At the peak of EAE score (day 21) when

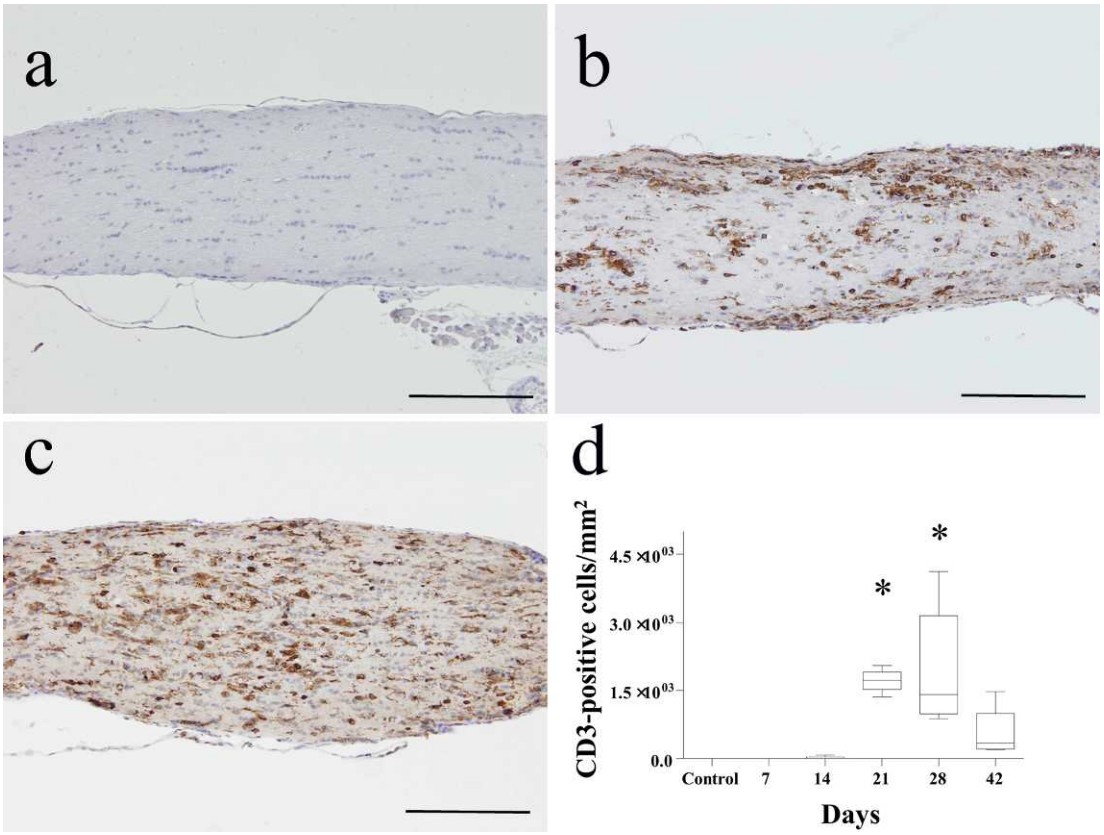

Figure 6. Immunohistochemical study of T cells (CD3-positive cells) in the optic nerve. (**a**) Normal optic nerve. (**b**) EAON on day 21 after immunization. T cells infiltrate mainly from the sheath of the optic nerve. (**c**) Optic nerve of an EAON model mouse on day 28 after immunization. T cell infiltration expands to the optic nerve parenchyma. *Bar* = 100 μm. (**d**) Chronological changes of number of T cells in the optic nerve. *Box-and-whisker plots* indicate median, range, upper quartile, and lower quartile obtained from five mice in each group. Statistical analysis was performed using Mann-Whitney *U* test. $^*P < 0.05$ compared to control.

paralysis was most severe, OKT threshold was the lowest (right eye: 0.127 ± 0.103 cyc/deg, left eye: 0.120 ± 0.098 cyc/deg), and VEP latency was the longest (70.00 ± 0.00 ms). As EAE score recovered from the peak, OKT threshold (Fig. 2: day 0: 0.413 ± 0.005 cyc/deg versus right eye: 0.132 ± 0.108 cyc/deg, left eye: 0.07 ± 0.058 cyc/deg) and VEP latency (Fig. 3: day 0: 43.74 ± 0.69 ms versus day 28: 55.78 ± 11.62 ms, day 42: 58.08 ± 10.01) also recovered but not to the normal levels.

Optokinetic tracking threshold is measured by monitoring the head and neck movement of the mouse in tracking the sinusoidal grating, in which the mouse has to use the forelimbs to stabilize the upper half of the body in order to move its neck. In the EAE–EAON model used in the present study, ascending muscle weakness starting from the tail spreading to the forelimbs could eventually influence the result of the OKT threshold, giving a worse result than the actual visual acuity of the mouse. To avoid this effect, our protocol excluded mice with an EAE score over 4.5 from this test. Furthermore, EAE score and OKT threshold were measured blindly by two experienced researchers on the same day. However, during the actual experiment, no mice had an EAE score exceeding 4.5, and therefore all mice were evaluated for OKT threshold.

Microglial Activation Precedes T Cell Infiltration and Demyelination

On day 14, before EAE score reached its peak, massive microglial activation in the optic nerve was observed (Fig. 4). In the normal optic nerve, microglia had long branched (ramified) processes (Fig. 4); whereas, in EAON, microglia appeared amoeboid with few short and thick processes (Fig. 4). Immunohistochemical study for Iba-1 confirmed that microglial activation started as early as day 14 in EAON (Fig. 4). Microglial activation involved not only expansion of microglia in number, but also a change in cell morphology into an activated state, suggesting that microglia play a role in the development of EAE–EAON. Neurofilament immunostaining of the optic nerve on day 14 showed partial irregularity of the linear neurofilament structure, which may represent the onset of axon damage. In the later phase, irregularly stained axons expanded throughout the optic nerve (Fig. 5). T cells started to infiltrate the optic nerve as early as day 14. Marked infiltration was observed in the optic nerve on days 21 to 28 and then subsided on day 42. T cells infiltrated from the sheath of the optic nerve on day 21 and then expanded into the optic nerve parenchyma on day 28 (Fig. 6). Myelin in the optic nerve was preserved on day 14, but areas of decreased MBP immunoreactivity in the optic nerve, which represent demyelination, were observed from day 21 (Fig. 7). In summary, marked microglial activation accompanied by onset of axon damage preceded T cell infiltration and demyelination in the optic nerve.

Correlation between Visual Function and Histopathology

Irregularity of neurofilaments, revealed by immunohistochemistry staining, was observed on day 14 (Fig. 5), when the OKT

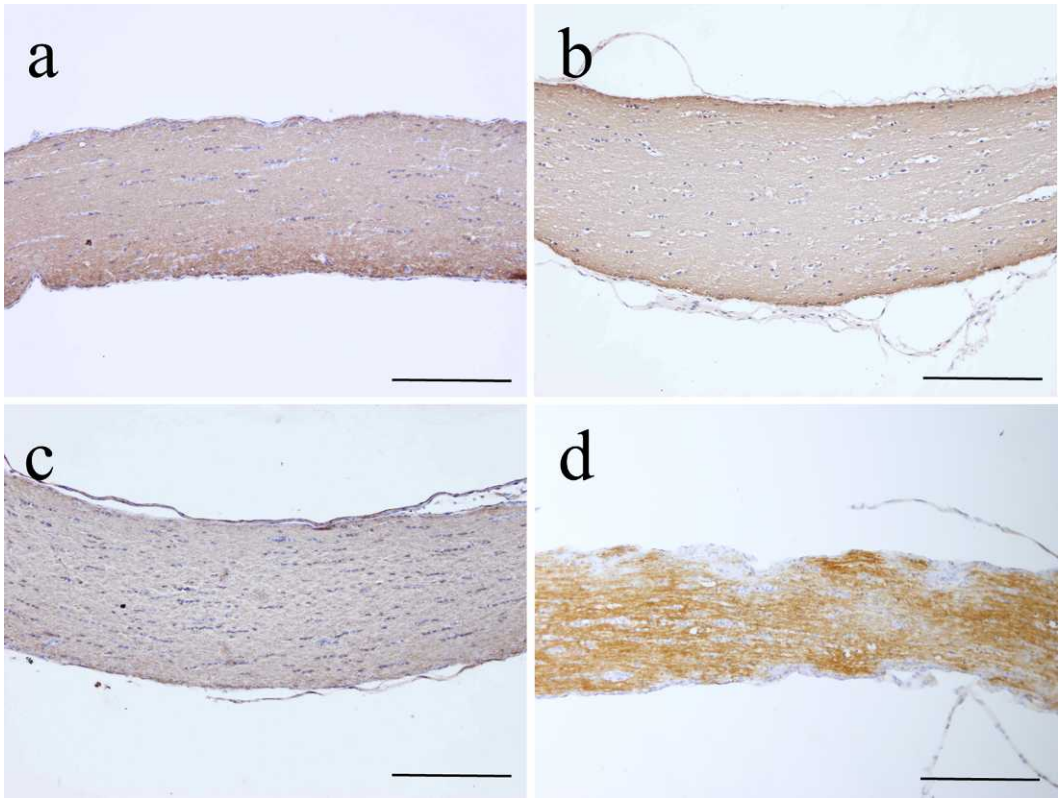

Figure 7. Immunohistochemical study of myelin basic protein (MBP) demonstrating demyelination of the optic nerve. (**a**) Normal optic nerve. Myelin is preserved in optic nerves of EAON model mice on day 7 (**b**) and day 14 after immunization (**c**). Decrease in immunostained surface area representing demyelination is observed in the optic nerve of an EAON mouse on day 21 after immunization (**d**). *Bar* = 200 μm.

threshold also declined (Fig. 2). At this time point, the predominate cells that infiltrated the optic nerve were not T cells but microglia (Fig. 4). This finding raised the possibility that microglia are the main effector cells that initiate axon damage and may have caused the decline in OKT threshold. On the contrary, on day 21, expansion of T cells in the optic nerve coincided with prolongation of VEP latency and demyelination (Fig. 7), which may explain the delay in conductivity in the optic nerve. From day 28 onward, infiltration of microglia and T cells subsided partially (Fig. 4), while OKT threshold and VEP latency also recovered but not to the normal levels.

Discussion

We investigated the relationship between histopathology of the optic nerve and visual function in a murine model of EAON from a chronological viewpoint. We found that the timing of decline in optic nerve function differed when assessed by OKT threshold and VEP latency, and the timing of decline in the two parameters coincided with different cell populations in the optic nerve. The decline in OKT threshold coincided with presumed axon damage, while the prolongation of VEP latency coincided with peak T cell infiltration. On the other hand, OKT threshold declined much earlier than VEP, and it coincided with microglial activation in the optic nerve. Although electrophysiological and histopathological studies of EAON have been reported, to the best of our knowledge, there is no report on the sequential changes of visual function and the corresponding histopathological findings during the course of EAON.

To understand the relation between optic nerve function and optic nerve pathology, a study using an EAON rat model proposes that VEP latency prolongation is the result of demyelination[20]; this is reasonable since myelin serves as an insulator, increasing the velocity of conduction of action potentials along myelinated axons compared to nonmyelinated fibers.[21] Studies using the EAE–EAON mouse model that we used in the present study suggest that MOG antigen–specific T cells are the main effector cells for inducing demyelination and axon pathology, which is similar in MS.[3,22,23] In our present study, we observed that demyelination coincided with VEP latency prolongation (day 21). Decline in the OKT threshold was observed from day 7 and reached the lowest point on day 21 (Fig. 2). The irregularity of neurofilament staining on day 14 (Fig. 5) may represent the onset of axon damage preceding demyelination, which may have led to the decline in the OKT threshold. In addition, worsening of the OKT threshold from day 14 to day 21 was observed when demyelination developed. This finding may indicate that the OKT threshold does not purely reflect axon pathology but is also related to demyelination to a certain degree.[3,24] In MS, even in white matter with normal appearance, axon loss exists without any demyelination, suggesting that axonal injury may develop from a mechanism independent from demyelination.[3,24,25] Although our results coincided with MS pathology, immunohistochemistry studies that use light microscopy have limitations for detecting axon damage. To detect subtle changes, the use of ultrastructural (Epon-embedded sections and electron microscopy) studies for myelin and axons may have revealed different results.

In our EAON model, the OKT threshold declined much earlier (day 14) than VEP prolongation (day 21), when microglial activation was present in the optic nerve but not

MOG-specific T cell infiltration (Figs. 2–4). Previous studies suggest that microglial activation in the spinal cord in EAE precedes clinical symptom onset and is followed by infiltration of T cells, causing demyelination.[11,12] The same sequence of events was also observed in our EAON model. The discrepancy between OKT threshold and VEP latency (conductivity) may reflect similar findings in human optic neuritis,[4,5] although one must keep in mind that neuronal circuitry is different between mice and humans: induction of optokinetic head tracking movement is a subcortical response and is not associated with the occipital lobe (V1) in mice.[26] The magnitude of OKT threshold induced has been reported to be influenced by the size of the image projected onto the retina,[26] indicating that the OKT threshold does not only reflect function of the optic nerve tract but is largely influenced by retinal ganglion cell function. Our result may represent early decline in retinal ganglion cell function secondary to optic nerve damage (visual field defect). To examine this hypothesis, electrophysiological studies in rodents, such as the scotopic threshold response, which indicates retinal ganglion cell function, are needed in future studies to elucidate the relationship between OKT and retinal ganglion cell function.

Early microglial activation has been suggested to play a crucial role in the development of EAE.[3,11,12] In our present study on optic neuritis, microglial activation also preceded T cell infiltration and coincided with decline in the OKT threshold, suggesting that microglial activation may have caused the initial damage to axons. The role of microglia in MS remains controversial. Microglia are known to play a detrimental role, secreting proinflammatory cytokines such as tumor necrosis factor (TNF)-α, interleukin (IL)-1β, and nitric oxide,[27,28] which can cause axon damage. At the same time, microglia have also been known to provide neuroprotection.[29] In a transgenic EAE model, suppression of microglia ameliorated EAE, suggesting that microglia play a major role in the development of EAE. In the present study, microglial activation might have caused a decline in OKT threshold, as implied from their temporal association. Tumor necrosis factor-α is another possible cause of axon damage. A recent study using a lipopolysaccharide-induced relapsing–remitting murine EAE model indicates that TNF-α production by systemic inflammation may cause axon degeneration.[30] We do not have direct evidence that microglia are responsible for deterioration in OKT threshold and axon pathology. Further experiments are needed to address this issue.

In a mouse EAE–EAON model, microglial infiltration in the optic nerve coincided with decline in the OKT threshold and preceded VEP latency prolongation; whereas VEP latency prolongation coincided with T cell infiltration and demyelination of the optic nerve. These findings may suggest that decline in OKT threshold is associated with microglial pathology in the acute phase and is further influenced by demyelination caused by T cell infiltration in a later phase. The understanding of this functional and histopathological relation may provide insight to develop new treatment strategies for optic neuritis.

Acknowledgments

The authors thank Masao Yoshikawa, Daigo Yoshikawa (Mayo Corporation), and Atsushi Mizota (Teikyo University) for technical advice on VEP measurements. We also thank Teresa Nakatani for critical revision of the manuscript.

References

1. Beck RW, Trobe JD, Moke PS, et al. High- and low-risk profiles for the development of multiple sclerosis within 10 years after optic neuritis: experience of the optic neuritis treatment trial. *Arch Ophthalmol*. 2003;121:944–949.
2. Frohman EM, Racke MK, Raine CS. Multiple sclerosis—the plaque and its pathogenesis. *N Engl J Med*. 2006;354:942–955.
3. Kornek B, Storch MK, Weissert R, et al. Multiple sclerosis and chronic autoimmune encephalomyelitis: a comparative quantitative study of axonal injury in active, inactive, and remyelinated lesions. *Am J Pathol*. 2000;157:267–276.
4. Jones SJ, Brusa A. Neurophysiological evidence for long-term repair of MS lesions: implications for axon protection. *J Neurol Sci*. 2003;206:193–198.
5. Jones SJ. Visual evoked potentials after optic neuritis. Effect of time interval, age and disease dissemination. *J Neurol*. 1993; 240:489–494.
6. Brusa A, Jones SJ, Plant GT. Long-term remyelination after optic neuritis: a 2-year visual evoked potential and psychophysical serial study. *Brain*. 2001;124:468–479.
7. Beck RW, Cleary PA. Optic neuritis treatment trial. One-year follow-up results. *Arch Ophthalmol*. 1993;111:773–775.
8. Shao H, Huang Z, Sun SL, Kaplan HJ, Sun D. Myelin/oligodendrocyte glycoprotein-specific T-cells induce severe optic neuritis in the C57BL/6 mouse. *Invest Ophthalmol Vis Sci*. 2004;45:4060–4065.
9. Kaushansky N, Zhong MC, Kerlero de Rosbo N, Hoeftberger R, Lassmann H, Ben-Nun A. Epitope specificity of autoreactive T and B cells associated with experimental autoimmune encephalomyelitis and optic neuritis induced by oligodendrocyte-specific protein in SJL/J mice. *J Immunol*. 2006;177: 7364–7376.
10. Chaudhary P, Marracci G, Yu X, Galipeau D, Morris B, Bourdette D. Lipoic acid decreases inflammation and confers neuroprotection in experimental autoimmune optic neuritis. *J Neuroimmunol*. 2011;233:90–96.
11. Ponomarev ED, Shriver LP, Maresz K, Dittel BN. Microglial cell activation and proliferation precedes the onset of CNS autoimmunity. *J Neurosci Res*. 2005;81:374–389.
12. Remington LT, Babcock AA, Zehntner SP, Owens T. Microglial recruitment, activation, and proliferation in response to primary demyelination. *Am J Pathol*. 2007;170:1713–1724.
13. McGill TJ, Douglas RM, Lund RD, Prusky GT. Quantification of spatial vision in the Royal College of Surgeons rat. *Invest Ophthalmol Vis Sci*. 2004;45:932–936.
14. Prusky GT, Alam NM, Beekman S, Douglas RM. Rapid quantification of adult and developing mouse spatial vision using a virtual optomotor system. *Invest Ophthalmol Vis Sci*. 2004;45:4611–4616.
15. Prusky GT, Douglas RM. Characterization of mouse cortical spatial vision. *Vision Res*. 2004;44:3411–3418.
16. Van Die GC, Collewijn H. Control of human optokinetic nystagmus by the central and peripheral retina: effects of partial visual field masking, scotopic vision and central retinal scotomata. *Brain Res*. 1986;383:185–194.
17. Shin YJ, Park KH, Hwang JM, Wee WR, Lee JH, Lee IB. Objective measurement of visual acuity by optokinetic response determination in patients with ocular diseases. *Am J Ophthalmol*. 2006;141:327–332.
18. Kezuka T, Usui Y, Goto H. Analysis of the pathogenesis of experimental autoimmune optic neuritis. *J Biomed Biotechnol*. 2011; doi:10.1155/2011/294046.
19. Heiduschka P, Schnichels S, Fuhrmann N, et al. Electrophysiological and histologic assessment of retinal ganglion cell fate in a mouse model for OPA1-associated autosomal dominant optic atrophy. *Invest Ophthalmol Vis Sci*. 2010;51:1424–1431.
20. You Y, Klistorner A, Thie J, Graham SL. Latency delay of visual evoked potential is a real measurement of demyelination in a rat model of optic neuritis. *Invest Ophthalmol Vis Sci*. 2011; 52:6911–6918.

21. Morell P, Roberson MD, Meissner G, Toews AD. Myelin: from electrical insulator to ion channels. *Prog Clin Biol Res*. 1990; 336:1–23.
22. Bielekova B, Sung MH, Kadom N, Simon R, McFarland H, Martin R. Expansion and functional relevance of high-avidity myelin-specific CD4+ T cells in multiple sclerosis. *J Immunol*. 2004;172:3893–3904.
23. Storch M, Lassmann H. Pathology and pathogenesis of demyelinating diseases. *Curr Opin Neurol*. 1997;10:186–192.
24. Bitsch A, Schuchardt J, Bunkowski S, Kuhlmann T, Bruck W. Acute axonal injury in multiple sclerosis. Correlation with demyelination and inflammation. *Brain*. 2000;123(pt 6);1174–1183.
25. Kuhlmann T, Lingfeld G, Bitsch A, Schuchardt J, Bruck W. Acute axonal damage in multiple sclerosis is most extensive in early disease stages and decreases over time. *Brain*. 2002;125: 2202–2212.
26. Wallman J. Subcortical optokinetic mechanisms. *Rev Oculomot Res*. 1993;5:321–342.
27. Viviani B, Bartesaghi S, Corsini E, Galli CL, Marinovich M. Cytokines role in neurodegenerative events. *Toxicol Lett*. 2004;149:85–89.
28. Chakfe Y, Seguin R, Antel JP, et al. ADP and AMP induce interleukin-1beta release from microglial cells through activation of ATP-primed P2X7 receptor channels. *J Neurosci*. 2002; 22:3061–3069.
29. Napoli I, Neumann H. Protective effects of microglia in multiple sclerosis. *Exp Neurol*. 2010;225:24–28.
30. Moreno B, Jukes JP, Vergara-Irigaray N, et al. Systemic inflammation induces axon injury during brain inflammation. *Ann Neurol*. 2011;70:932–942.